

Helical temperature perturbations associated with tearing modes in tokamak plasmas

Richard Fitzpatrick

Citation: [Physics of Plasmas \(1994-present\)](#) **2**, 825 (1995); doi: 10.1063/1.871434

View online: <http://dx.doi.org/10.1063/1.871434>

View Table of Contents: <http://scitation.aip.org/content/aip/journal/pop/2/3?ver=pdfcov>

Published by the [AIP Publishing](#)

Articles you may be interested in

[Fast growing double tearing modes in a tokamak plasma](#)

Phys. Plasmas **12**, 082504 (2005); 10.1063/1.1989727

[Stability of tearing modes in tokamak plasmas](#)

Phys. Plasmas **1**, 2308 (1994); 10.1063/1.870628

[Turbulent stabilization of the tearing mode in tokamak plasmas](#)

Phys. Fluids **29**, 200 (1986); 10.1063/1.865977

[Turbulence driven tearing modes in a tokamak plasma](#)

Phys. Fluids **24**, 1303 (1981); 10.1063/1.863521

[Tearing mode in the cylindrical tokamak](#)

Phys. Fluids **16**, 1054 (1973); 10.1063/1.1694467



PFEIFFER VACUUM

VACUUM SOLUTIONS FROM A SINGLE SOURCE

Pfeiffer Vacuum stands for innovative and custom vacuum solutions worldwide, technological perfection, competent advice and reliable service.



Helical temperature perturbations associated with tearing modes in tokamak plasmas

Richard Fitzpatrick

Institute for Fusion Studies, The University of Texas at Austin, Austin, Texas 78712

(Received 12 September 1994; accepted 28 November 1994)

An investigation is made into the electron temperature perturbations associated with tearing modes in tokamak plasmas. It is found that there is a critical magnetic island width below which the conventional picture where the temperature is flattened inside the separatrix is invalid. This effect comes about because of the *stagnation* of magnetic field lines in the vicinity of the rational surface and the *finite* parallel thermal conductivity of the plasma. Islands whose widths lie below the critical value are not destabilized by the perturbed bootstrap current, unlike conventional magnetic islands. This effect may provide an explanation for some puzzling experimental results regarding error field-induced magnetic reconnection. The critical island width is found to be fairly substantial in conventional tokamak plasmas, provided that the long mean-free path nature of parallel heat transport and the anomalous nature of perpendicular heat transport are taken into account in the calculation. © 1995 American Institute of Physics.

I. INTRODUCTION

Oscillatory low mode number helical perturbations of the magnetic field, temperature, and density are often observed in tokamak plasmas, especially during the current ramp-up and ramp-down phases.¹⁻³ These perturbations are usually identified as a type of filamentation instability of the plasma current known as a “tearing mode.”⁴ A saturated tearing mode is expected to form a magnetic island structure that locally flattens the plasma temperature and density profiles, thereby degrading the overall energy and particle confinement.^{5,6} In general, the island rotates in the laboratory frame due to the presence of a radial electric field in the plasma. Diamagnetic effects also give rise to island rotation. The uncontrolled growth of tearing islands with different helicities is predicted to give rise to rapid stochasticization of the magnetic field, with an associated catastrophic loss of confinement.^{7,8} For many decades, tearing mode theory has provided a fairly good *qualitative* explanation for most large-scale instabilities observed in tokamak plasmas.⁹ Unfortunately, no conclusive *quantitative* comparison between theory and experiment has ever been performed, mainly because of the great difficulty of accurately measuring the internal (i.e., inside the plasma) structure of tearing modes.

Magnetic pickup coils located outside the plasma yield little detailed information about the internal structure of tearing instabilities.¹⁰ Generally speaking, the equilibrium current profile is not known to sufficient accuracy to permit the projection of edge measurements back into the plasma with any degree of certainty.

The internal structure of tearing modes can be investigated more directly using soft X-ray (SXR) emission data.¹¹ Unfortunately, SXR observations are generally restricted to the plasma core (i.e., well inside the $q=2$ surface) and are, of course, chord averaged. Tomographic reconstruction of the emission profile is possible, but, in practice, extremely difficult to achieve.^{12,13}

An electron cyclotron emission (ECE) detector gives a direct *localized* measurement of the electron temperature at a

known and adjustable position inside the plasma.^{11,13} Clearly, this diagnostic has far greater potential for probing the internal structure of tearing instabilities than either a magnetic pickup coil array or a SXR detector. The aim of this paper is to establish the relationship between the magnetic structure of a saturated tearing mode and the associated helical perturbation of the electron temperature profile. It is demonstrated in Sec. III that this information can be used, in conjunction with experimental ECE data, to determine the structure throughout the plasma. It is also shown that a temperature flattened magnetic island possesses a *unique* ECE signature. The heat flow pattern around such an island is calculated in Sec. IV. The effect of the perturbed bootstrap current on island stability, taking into account the finite parallel thermal conductivity of the plasma, is investigated in Sec. V. In Sec. VI we discuss the implications of some of the results obtained in this paper for Ohmically heated tokamaks. Finally, some important conclusions are drawn in Sec. VII.

II. BASIC TEARING MODE THEORY

A. The plasma equilibrium

The analysis is performed in cylindrical geometry with the usual right-handed polar coordinates (r, θ, z) . The equilibrium magnetic field is written as $\mathbf{B} \equiv [0, B_\theta(r), B_z]$, where B_z is the constant “toroidal” field strength. The equilibrium “toroidal” current density takes the form $\mu_0 J_z(r) \equiv (r B_\theta)'/r$, where $'$ denotes d/dr . It is convenient to define the “safety factor” $q(r) = r B_z / R_0 B_\theta$, where $2\pi R_0$ is the assumed periodicity length in the z direction (R_0 is the simulated major radius). The standard large aspect ratio tokamak orderings, $B_\theta/B_z \ll 1$ and $r/R_0 \ll 1$, are adopted.¹⁴

B. The outer region

Consider a saturated tearing instability with m periods in the poloidal direction and n periods in the “toroidal” direc-

tion. The perturbed magnetic field is written in the usual manner as $\delta\mathbf{B} = \nabla(\psi/\hat{z}) \equiv \nabla\psi/\hat{z}$, where the perturbed poloidal flux ψ takes the general form

$$\psi(r, \theta, z, t) = \psi(r) \cos \zeta. \quad (1)$$

Here,

$$\zeta = m\theta - n \frac{z}{R_0} - \int^t \omega(t') dt' \quad (2)$$

is the helical phase angle of the mode, and $\omega(t)$ is its instantaneous rotation frequency.

According to ideal magnetohydrodynamics (MHD) (i.e., linearized force balance in an incompressible, inviscid, massless, perfectly conducting fluid), the magnetic perturbation obeys

$$\frac{1}{r} \frac{d}{dr} \left(r \frac{d\psi}{dr} \right) - \frac{m^2}{r^2} \psi - \frac{\mu_0 J'_z}{B_\theta (1 - q/q_s)} \psi = 0 \quad (3)$$

in cylindrical geometry, where $q_s \equiv q(r_s) = m/n$ defines the position of the “rational” flux surface.¹⁵ In ideal MHD theory, a tearing mode is simply an incompressible helical displacement ξ of the equilibrium magnetic flux surfaces. The radial displacement is written as

$$\xi_r = \xi(r) \cos \zeta, \quad (4)$$

where

$$\xi(r) = \frac{\psi(r)}{B_\theta (1 - q/q_s)}. \quad (5)$$

C. The magnetic island

In the vicinity of the rational surface,

$$\psi(r) \approx \Psi \quad (6)$$

for tearing instabilities, where $\Psi > 0$ is termed the “reconnected flux.” Equation (6) is equivalent to the well-known “constant- ψ ” approximation.⁴ In principle, if $\Psi \neq 0$, both Eqs. (3) and (5) become singular as $r \rightarrow r_s$. Unphysical behavior is averted by the formation of a magnetic island.

It is convenient to define the “helical flux,”¹⁶

$$\chi(r, \zeta) = - \int_{r_s}^r \left(1 - \frac{q}{q_s} \right) B_\theta dr + \psi(r) \cos \zeta. \quad (7)$$

It is easily demonstrated that $(\mathbf{B} + \delta\mathbf{B}) \cdot \nabla \chi = 0$, so the contours of χ map out the perturbed magnetic flux surfaces. Close to the rational surface, Eqs. (6) and (7) yield

$$\Omega = \frac{\chi}{\Psi} = 8 \frac{x^2}{W^2} + \cos \zeta, \quad (8)$$

where $x = r - r_s$, and

$$W = 4 \sqrt{\frac{R_0 q_s}{B_z s_s}} \Psi. \quad (9)$$

Here, $s_s = (rq'/q)_{r_s}$ is the local magnetic shear, which is assumed to be positive.

Figure 1 shows contours of the normalized flux surface label Ω plotted in (x, ζ) space. An island structure of maximum radial width W is clearly evident. The island O point

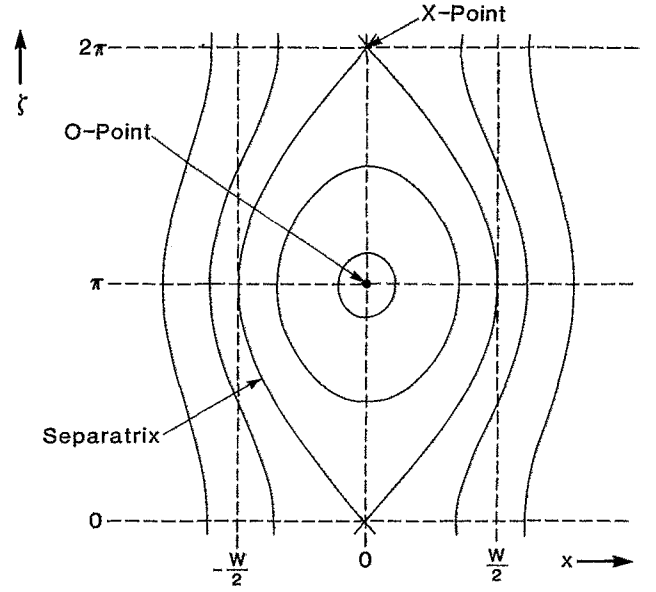


FIG. 1. Contours of the normalized flux surface label Ω plotted in (x, ζ) space, where x is the radial distance from the rational surface and ζ is the helical angle.

lies at coordinates $(\Omega = -1, \zeta = \pi)$, the separatrix corresponds to the $\Omega = 1$ contour, and the X point is situated at coordinates $(\Omega = 1, \zeta = 0)$. The perturbed flux surfaces are, of course, periodic in the helical phase angle ζ , repeating every 2π rads.

III. THE PERTURBED TEMPERATURE PROFILE

A. Introduction

Heat flow in the plasma is governed by¹⁷

$$\mathbf{q} = -\kappa_{\parallel} \nabla_{\parallel} T - \kappa_{\perp} \nabla_{\perp} T, \quad (10)$$

where \mathbf{q} is the heat flux, T is the (single fluid) temperature, κ_{\parallel} and κ_{\perp} is the parallel and perpendicular thermal conductivities, respectively, and

$$\begin{aligned} \nabla_{\parallel} T &\equiv (\mathbf{b} \cdot \nabla T) \mathbf{b}, \\ \nabla_{\perp} T &\equiv \nabla T - \nabla_{\parallel} T, \end{aligned} \quad (11)$$

with $\mathbf{b} \equiv \mathbf{B}/|B| \approx \mathbf{B}/B_z$. Note that $\nabla \cdot \mathbf{b} \approx 0$ in a large aspect ratio tokamak.

In regions of the plasma where there are no significant sources or sinks of heat (i.e., everywhere apart from the plasma core and the scrape-off layer),

$$\nabla \cdot \mathbf{q} = 0, \quad (12)$$

so Eq. (10) yields

$$\kappa_{\parallel} \nabla_{\parallel}^2 T + \kappa_{\perp} \nabla_{\perp}^2 T = 0 \quad (13)$$

(assuming that κ_{\parallel} and κ_{\perp} are constants, for the sake of simplicity), where

$$\begin{aligned} \nabla_{\parallel}^2 T &\equiv \mathbf{b} \cdot \nabla (\mathbf{b} \cdot \nabla T), \\ \nabla_{\perp}^2 T &\equiv \nabla^2 T - \nabla_{\parallel}^2 T. \end{aligned} \quad (14)$$

In the vicinity of the rational surface,

$$\mathbf{b} \cdot \nabla \approx - \left(\frac{ns_s}{R_0 r_s} \right) x \frac{\partial}{\partial \zeta} \Big|_{\Omega}, \quad (15a)$$

$$\nabla_{\perp}^2 \approx \hat{\mathbf{r}} \frac{\partial^2}{\partial x^2} \Big|_{\zeta}, \quad (15b)$$

in the thin island limit $W \ll r_s$, so for a resonant perturbation (i.e., $\delta T \sim 1/x$) the first term in Eq. (13) dominates the second whenever

$$|x| \gg x_c \sim \left(\frac{\kappa_{\perp}}{\kappa_{\parallel}} \right)^{1/4} \left(\frac{R_0 r_s}{ns_s} \right)^{1/2}. \quad (16)$$

Thus, far from the rational surface (i.e., $|x| \gg x_c$), the parallel thermal conductivity forces the temperature to be a function of the perturbed flux surfaces. Conversely, the temperature is not necessarily a flux surface function close to the rational surface.

B. The outer region

In the outer region (i.e., $|x| \gg x_c$, W) a tearing perturbation reduces to a helical displacement of the magnetic flux surfaces, and the temperature remains a function of these surfaces. Let $T_0(r)$ be the unperturbed equilibrium temperature profile. It follows that the temperature perturbation associated with a tearing mode is given by

$$\delta T(r, \zeta) = -\nabla T_0 \cdot \xi = \delta T(r) \cos \zeta, \quad (17)$$

where

$$\delta T(r) = -T'_0(r) \xi(r). \quad (18)$$

C. The island region

Let

$$T(r, \zeta) = T_0(r_s) + \tilde{T}(x, \zeta), \quad (19)$$

in the vicinity of the island. To lowest order, the function \tilde{T} is antisymmetric about the rational surface,

$$\tilde{T}(-x, \zeta) = -\tilde{T}(x, \zeta), \quad (20)$$

since it satisfies the antisymmetric boundary condition,

$$\tilde{T}(x, \zeta) = T'_s x + \frac{WT'_s}{16} \frac{W}{x} \cos \zeta, \quad (21)$$

for $W \ll |x| \ll r_s$ [see Eqs. (5), (9), and (18)]. Here, $T'_s \equiv T'_0(r_s)$ is the local equilibrium temperature gradient. The island temperature profile is assumed to be symmetric about the O point,

$$\tilde{T}(x, -\zeta) = \tilde{T}(x, \zeta), \quad (22)$$

and periodic in the helical phase angle,

$$\tilde{T}(x, \zeta + 2\pi) = \tilde{T}(x, \zeta). \quad (23)$$

Close to the magnetic island, the heat diffusion equation (13) is conveniently written as

$$\frac{1}{4} \left[\left(\frac{W}{W_c} \right)^2 \sin \zeta \frac{\partial}{\partial X} + X \frac{\partial}{\partial \zeta} \right]^2 \tilde{T} + \frac{\partial^2 \tilde{T}}{\partial X^2} = 0, \quad (24)$$

where

$$X = 4 \frac{x}{W_c}. \quad (25)$$

Equation (13) can also be written as

$$\frac{1}{4} \left(\frac{W}{W_c} \right)^4 \frac{\partial}{\partial \zeta} \sqrt{\Omega - \cos \zeta} \frac{\partial \tilde{T}}{\partial \zeta} + \frac{\partial}{\partial \Omega} \sqrt{\Omega - \cos \zeta} \frac{\partial \tilde{T}}{\partial \Omega} = 0. \quad (26)$$

In Eqs. (25) and (26), the scale island width W_c is defined as

$$\frac{W_c}{r_s} = \sqrt{8} \left(\frac{\kappa_{\perp}}{\kappa_{\parallel}} \right)^{1/4} \left(\frac{1}{\epsilon_s s_s n} \right)^{1/2}, \quad (27)$$

where $\epsilon_s = r_s/R_0$. Clearly, W_c is closely related to the quantity x_c defined in Eq. (16).

D. The small island limit

Consider the small island limit, $W \ll W_c$, for which the temperature is not a function of island flux surfaces according to Eqs. (16) and (27). Suppose that

$$\tilde{T}(X, \zeta) = \sum_{\nu=0}^{\infty} \tilde{T}_{\nu}(X) \cos \nu \zeta, \quad (28)$$

where ν is an integer. This automatically satisfies the symmetry requirements (22) and (23). It follows from the expansion of Eq. (24) in the small parameter $(W/W_c)^2$ that

$$\begin{aligned} \frac{d^2 \tilde{T}_0}{dX^2} &\approx 0, \\ \frac{d^2 \tilde{T}_1}{dX^2} - \frac{X^2}{4} \tilde{T}_1 &\approx -\frac{1}{4} \left(\frac{W}{W_c} \right)^2 X \frac{d\tilde{T}_0}{dX} \end{aligned} \quad (29)$$

to lowest order, where

$$\frac{\tilde{T}_{\nu}}{\tilde{T}_0} \sim \mathcal{O} \left(\frac{W}{W_c} \right)^{2\nu}. \quad (30)$$

Application of the boundary condition (21) yields

$$\tilde{T}_0 \approx \frac{W_c T'_s}{4} X \quad (31)$$

and

$$\tilde{T}_1 \approx \frac{WT'_s}{16} \frac{W}{W_c} f(X), \quad (32)$$

where

$$\frac{d^2 f}{dy^2} - \frac{y^2}{4} f = -y. \quad (33)$$

The physical constraints on the solution of Eq. (33) are $f(0) = 0$, and $f \rightarrow 0$ as $|y| \rightarrow \infty$. Figure 2 shows $f(y)$ evaluated numerically in the region $y \geq 0$. The function reaches a maximum value $f_{\max} \approx 1.44$ at $y \approx 2$. For $y \ll 2$,

$$f(y) \approx 1.2y, \quad (34)$$

and for $y \gg 2$,

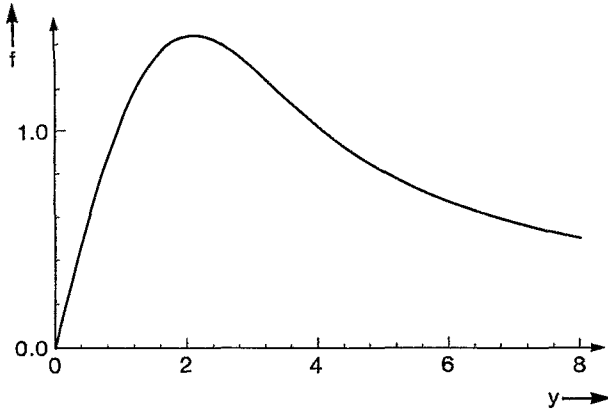


FIG. 2. The function $f(y)$ that characterizes the helical temperature perturbation around a thin island for which the temperature is not a flux surface function [see Eqs. (32)–(35)].

$$f(y) \approx \frac{4}{y}. \quad (35)$$

In the small island limit, $W \ll W_c$, the perturbed temperature is “linear” throughout the plasma [i.e., it is everywhere dominated by the principal ($\nu=1$) harmonic]. According to Eq. (30), the overtone harmonics ($\nu>1$) are smaller than the principal harmonic by at least a factor $(W/W_c)^2$. In the outer region,

$$\begin{aligned} \delta T(r, \zeta) &\equiv T(r, \zeta) - T_0(r) \\ &\approx \frac{W^2}{16} T'_0(r) \frac{s_s}{r} \frac{q/q_s}{q/q_s - 1} \hat{\psi}(r) \cos \zeta, \end{aligned} \quad (36)$$

where use has been made of Eqs. (5), (9), (17), and (18). Here, $\hat{\psi}(r)$ is a solution of the cylindrical tearing mode equation (3) (for the m/n mode), subject to the normalizing condition $\hat{\psi}(r_s) = 1$. In the vicinity of the rational surface,

$$\delta T(x, \zeta) \approx 1.2 \frac{WT'_s}{4} \frac{W}{W_c} \frac{x}{W_c} \cos \zeta, \quad (37)$$

for $|x| \ll W_c/2$, and

$$\delta T(x, \zeta) \approx \frac{WT'_s}{16} \frac{W}{x} \cos \zeta, \quad (38)$$

for $|x| \gg W_c/2$. Note that Eq. (36) connects smoothly onto Eq. (38) for $W_c/2 \ll |x| \ll r_s$.

E. The large island limit

In the large island limit, $W \gg W_c$, the temperature is a function of the island flux surfaces according to Eq. (26), so

$$\tilde{T} = \tilde{T}(\Omega). \quad (39)$$

On flux surfaces situated inside the separatrix ($\Omega < 1$), Eqs. (20) and (39) imply that $\tilde{T} = 0$, giving the well-known result that the temperature is flattened within the island separatrix.¹⁸ On flux surfaces outside the separatrix, Eq. (26) can be averaged over the helical phase angle ζ , to give

$$\frac{d}{d\Omega} \left(\oint \sqrt{\Omega - \cos \zeta} \frac{d\zeta}{2\pi} \frac{d\tilde{T}}{d\Omega} \right) = 0, \quad (40)$$

where use has been made of the periodicity constraint (23). Equation (40) and the boundary condition (21) yield¹⁹

$$\begin{aligned} \frac{d\tilde{T}}{d\Omega} &= \pm \frac{WT'_s}{\sqrt{32}} \bigg/ \oint \sqrt{\Omega - \cos \zeta} \frac{d\zeta}{2\pi} \\ &= \pm \frac{\pi}{16} \frac{WT'_s}{kE(1/k^2)}, \end{aligned} \quad (41)$$

for $\Omega \geq 1$, where $k = \sqrt{(1 + \Omega)/2}$,

$$E(l) = \int_0^{\pi/2} \sqrt{1 - l^2 \sin^2 \alpha} d\alpha, \quad (42)$$

is a standard elliptic integral,²⁰ and the \pm signs denote $x \geq 0$, respectively.

The perturbed temperature close to the island is conveniently written as

$$\delta T(x, \zeta) = \sum_{\nu=1}^{\infty} \delta T_{\nu}(x) \cos \nu \zeta, \quad (43)$$

where ν is an integer. It follows from Eqs. (19) and (36) that

$$\delta T_{\nu}(x) = 2 \oint \tilde{T}(x, \zeta) \cos \nu \zeta \frac{d\zeta}{2\pi}, \quad (44)$$

where the integration is performed at constant x . Integration by parts gives

$$\delta T_{\nu}(x) = \pm \frac{WT'_s}{16\nu} \int_0^{\zeta_c} \frac{\cos(\nu-1)\zeta - \cos(\nu+1)\zeta}{kE(1/k^2)} d\zeta, \quad (45)$$

where use has been made of Eq. (41). Here,

$$\zeta_c = \cos^{-1}(1 - 8x^2/W^2) \quad (46)$$

for $|x| < W/2$, $\zeta_c = \pi$ for $x \geq W/2$, and

$$k = \sqrt{\cos^2 \frac{\zeta}{2} + 4 \frac{x^2}{W^2}}. \quad (47)$$

In the asymptotic limit $|x| \gg W/2$, Eq. (45) yields

$$\delta T_1(x) \approx \frac{WT'_s}{16} \frac{W}{x}, \quad (48)$$

$$\delta T_{\nu>1}(x) \approx WT'_s \times \mathcal{O}\left[\left(\frac{W}{x}\right)^3\right].$$

In the opposite limit, $|x| \ll W/2$, Eq. (45) reduces to

$$\delta T_{\nu}(x) \approx \frac{8}{3} WT'_s \left(\frac{x}{W}\right)^3. \quad (49)$$

Note that Eqs. (43) and (48) match smoothly to the outer solution (36), when $W/2 \ll |x| \ll r_s$.

Figure 3 shows $\delta \hat{T}_{\nu}(x) \equiv \delta T_{\nu}(x)/WT'_s$ for $\nu=1-4$. It can be seen that inside the separatrix the overtone harmonics ($\nu>1$) are almost as large as the principal harmonic ($\nu=1$). In this respect, the perturbed temperature is “nonlinear” in the island region. The overtone harmonics die away rapidly

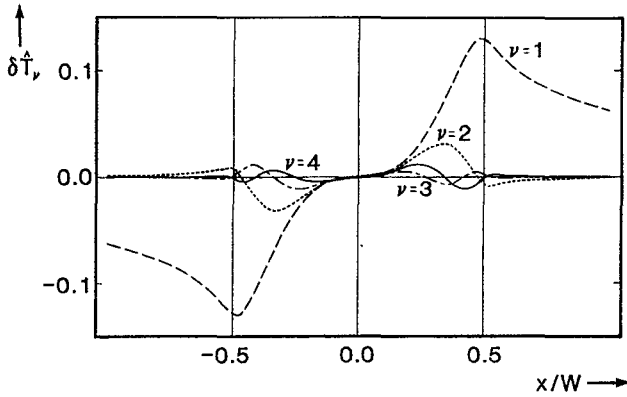


FIG. 3. The potentials δT_ν plotted as functions of the radial distance from the rational surface x , for ν in the range 1–4. The δT_ν characterize the helical temperature perturbation around a large island for which the temperature is a flux surface function [see Eqs. (43)–(45)].

for $|x| > W/2$. Thus, the observation of a localized overtone harmonic content of the perturbed temperature (using an ECE diagnostic) is an unambiguous indication of the presence of a pressure flattened magnetic island. (Recall from the previous section that an island that does not flatten the temperature profile leads to virtually no overtone harmonics content of the perturbed temperature.) The radial extent of the region of significant overtone harmonics is a good measure of the island width.

F. Discussion

In the outer region ($|x| \gg W, W_c$), the temperature measured by an ECE diagnostic focused on plasma located at coordinates (r_c, θ_c, z_c) can be written as

$$T(t) \approx T_0(r_c) + \delta T(r_c) \cos(m\theta_c - nz_c/R_0 - \omega t - \zeta_0), \quad (50)$$

in the presence of a *uniformly rotating* (m/n) tearing mode. Here, ζ_0 is an arbitrary (constant) phase angle. Clearly, both $T_0(r_c)$ and $\delta T_0(r_c)$ can be determined by observing the temperature variations over many rotation periods. The profiles $T_0(r)$ and $\delta T(r)$ can be evaluated using an array of ECE detectors tuned to slightly different frequencies³ or, alternatively, by sweeping the cyclotron resonance position by slowly ramping the toroidal field strength²¹ (the toroidal current must also be ramped in order to keep the edge- q constant). According to Eq. (18) the displacement eigenfunction in the outer region is given by

$$\xi(r) = \frac{\delta T(r)}{-T'_0(r)}. \quad (51)$$

The poloidal flux eigenfunction takes the form

$$\psi(r) = \frac{\mu_0 I_p}{2\pi a} \left(\frac{q_a}{q} - \frac{q_a}{q_s} \right) \xi(r) \quad (52)$$

[see Eq. (5)], where a is the plasma minor radius, q_a is the edge safety factor, and I_p is the total equilibrium “toroidal” plasma current. The displacement eigenfunction can clearly be constructed directly from ECE measurements. However, the construction of the flux eigenfunction requires a knowl-

edge of the safety factor profile. Fortunately, the accuracy to which the q profile must be determined is far less than that needed to solve the cylindrical tearing mode (3) directly. The crucial point is that the direct solution of Eq. (3) requires a knowledge of the current gradient profile, which depends on the *second derivative* of the q profile, and is, consequently, extremely difficult to determine accurately from experimental data.

If the island width is much less than the scale width W_c [see Eq. (27)], then there is no flattening of the temperature profile, and Eq. (50) is valid in the inner region ($|x| \ll W_c$). The perturbed temperature profile $\delta T(r)$ is antisymmetric about the rational surface, reaching local extrema of amplitude,

$$\delta T_{\text{ext}} \approx 0.09 W |T'_s| \frac{W}{W_c}, \quad (53)$$

at $r_\pm \approx r_s \pm W_c/2$ (see Sec. III D). Thus, the island width W is given by

$$W \approx \left(\frac{\delta T_{\text{ext}}(r_+ - r_-)}{0.09 |T'_s|} \right)^{1/2}. \quad (54)$$

If the island width is much greater than the scale width W_c , then the temperature profile is flattened inside the separatrix and

$$T(t) = T_0(r_s) + \tilde{T}_0(r_c) + \sum_{\nu=1}^{\infty} \delta T_\nu(r_c) \cos[\nu(m\theta_c - nz_c/R_0 - \omega t - \zeta_0)], \quad (55)$$

in the vicinity of the rational surface (see Secs. III D and III E), where $\tilde{T}_0(r) \rightarrow T'_s(r - r_s)$ and $\delta T_{\nu>1}(r)/\delta T_1(r) \rightarrow 0$ for $r_s \gg |r - r_s| \gg W/2$. Thus, the presence of overtone harmonics $\delta T_{\nu>1}$ localized close to the rational surface is an unambiguous indication of the existence of a magnetic island that flattens the temperature profile.²² The principal harmonic profile $\delta T_1(r)$ is antisymmetric about the rational surface (as are the overtone harmonic profiles), reaching local extrema of amplitude

$$\delta T_{1 \text{ ext}} \approx 0.13 W |T'_s|, \quad (56)$$

at $r_\pm \approx r_s \pm W/2$. Thus, the island width W is given by

$$W \approx \frac{\delta T_{1 \text{ ext}}}{0.13 |T'_s|}. \quad (57)$$

The (temporal) Fourier analysis of ECE data $T(t)$ produced by a plasma containing a *nonuniformly* rotating tearing mode (e.g., a large mode in the presence of a field error) can produce spurious overtone harmonics.³ However, these signals can easily be distinguished from the overtones associated with temperature flattening, because they are *nonlocalized*. In fact, in this case the nonlinear distortions seen on ECE data emanating from inside the plasma ought to match those seen using magnetic pickup coils.

IV. HEAT FLOW ACROSS A LARGE ISLAND

A. Introduction

The large island model outlined in the first paragraph of Sec. III E has been widely discussed in the literature.^{5,18} Unfortunately, as it stands, this model possesses one extremely unsatisfactory feature. Outside the separatrix there is a finite heat flux flowing across magnetic surfaces, driven by the cross-surface temperature gradient, whereas inside the separatrix there is zero heat flux because the temperature profile is flat. The model offers no explanation for how heat is transported from one side of the island to the other. In the following, it is demonstrated that the heat is actually transported along a boundary layer located on the island separatrix, and flows across the rational surface in the vicinity of the X points.

B. The boundary layer on the separatrix

Consider the limit $W \gg W_c$. Let

$$\Omega = 1 + 4 \left(\frac{W_c}{W} \right)^2 y, \quad (58)$$

$$\mu = \cos(\zeta/2),$$

then Eq. (26) reduces to

$$\frac{\partial}{\partial \mu} (1 - \mu^2) \frac{\partial \tilde{T}}{\partial \mu} + \frac{\partial^2 \tilde{T}}{\partial y^2} = 0, \quad (59)$$

on the separatrix [i.e., $y \sim \mathcal{O}(1)$], well away from the X points (i.e., $\sqrt{1 - \mu^2} \gg W_c/W$). In the region $x > 0$, the boundary conditions are

$$\tilde{T}(y, \mu) \rightarrow \frac{\pi}{4} W T'_s \left(\frac{W_c}{W} \right)^2 y, \quad (60)$$

as $y \rightarrow \infty$ and $\tilde{T} \rightarrow 0$ as $y \rightarrow -\infty$ (see Sec. III E).

Suppose that

$$\tilde{T}(y, \mu) = \frac{\pi}{8} W T'_s \left(\frac{W_c}{W} \right)^2 [y + |y| + \hat{T}(y, \mu)], \quad (61)$$

where

$$\begin{aligned} \hat{T}(-y, \mu) &= \hat{T}(y, \mu), \\ \hat{T}(y, -\mu) &= \hat{T}(y, \mu), \end{aligned} \quad (62)$$

with

$$\frac{\partial \hat{T}(y, \mu)}{\partial y} \rightarrow 0 \quad (63)$$

as $y \rightarrow \infty$, and

$$\frac{\partial \hat{T}(0, \mu)}{\partial y} = -1. \quad (64)$$

It follows that $\tilde{T}(y, \mu)$ satisfies all of the physical boundary conditions, plus the symmetry requirement (22), and is continuous up to and including its second derivatives.

The function $\hat{T}(y, \mu)$ satisfies Eq. (59). This equation can be solved by separation of variables to give the general expression

$$\begin{aligned} \hat{T}(y, \mu) &= - \sum_{l=1}^{\infty} \frac{a_l}{\sqrt{2l(2l-1)}} Q_{2l-1}(\mu) \\ &\quad \times \exp[-\sqrt{2l(2l-1)}|y|] \\ &\quad + \sum_{l=1}^{\infty} \frac{b_l}{\sqrt{2l(2l+1)}} P_{2l}(\mu) \\ &\quad \times \exp[-\sqrt{2l(2l+1)}|y|], \end{aligned} \quad (65)$$

which satisfies all of the above constraints, provided

$$\sum_{l=1}^{\infty} [b_l P_{2l}(\mu) - a_l Q_{2l-1}(\mu)] = 1. \quad (66)$$

Here, the P_j and the Q_j are standard Legendre functions (where j is an integer).²³ Note that Eq. (66) can be satisfied by choosing the a_l , such that

$$\sum_{l=1}^{\infty} a_l Q_{2l-1}(\mu) = -1, \quad (67)$$

in which case the well-known orthogonality property of the P_j functions yields $b_l = 0$ for all $l \geq 1$. Now,²⁴

$$\int_{-1}^1 Q_{2l-1}(\mu) P_{2k}(\mu) d\mu = \frac{-1}{2(l-k-1/2)(l+k)}, \quad (68a)$$

$$\int_{-1}^1 P_{2k}(\mu) d\mu = 2\delta_{k0}, \quad (68b)$$

so Eq. (67) reduces to

$$\sum_{l=1}^{\infty} \frac{a_l}{4(l-k-1/2)(l+k)} = \delta_{k0}, \quad (69)$$

for $k = 0, 1, 2, \dots$.

Consider the behavior in the vicinity of the X points, which are located at $y = 0$ and $\mu = \pm 1$. Close to $|\mu| = 1$,²⁴

$$\begin{aligned} Q_{2l-1}(\mu) &\approx -[\ln \sqrt{1 - \mu^2} + \gamma - \ln 2 + \psi(2l)], \\ P_{2k}(\mu) &\approx 1, \end{aligned} \quad (70)$$

where γ is Euler's constant and ψ is a standard digamma function.²⁵ It follows that as $|\mu| \rightarrow 1$,

$$\tilde{T}(y=0, \mu) \rightarrow \frac{\pi}{8} W T'_s \left(\frac{W_c}{W} \right)^2 A (\ln \sqrt{1 - \mu^2} + B), \quad (71)$$

where

$$A = \sum_{l=1}^{\infty} \frac{a_l}{\sqrt{2l(2l-1)}}, \quad (72)$$

$$B = \gamma - \ln 2 + A^{-1} \sum_{l=1}^{\infty} \frac{a_l \psi(2l)}{\sqrt{2l(2l-1)}}.$$

Suppose that the summations in Eqs. (69) and (72) are truncated at $l = l_{\max}$. Equation (69) then becomes an

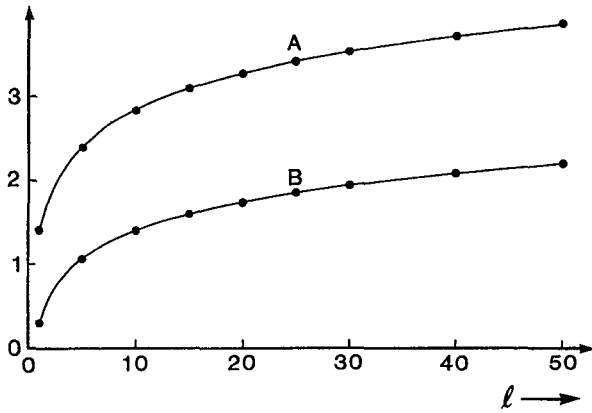


FIG. 4. The points show the truncated series A and B evaluated as functions of the number of terms l . The curves show the fits $A=1.401+0.626 \ln l$ and $B=0.296+0.482 \ln l$. The series A and B characterize the asymptotic matching of the boundary layer on the island separatrix to the X-point region [see Eqs. (71) and (72)].

$l_{\max} \times l_{\max}$ matrix equation that can easily be inverted numerically to give the a_l for $l=1$ to l_{\max} . The a_l can then be summed, with the weights specified in Eqs. (72), to give the parameters A and B . Figure 4 shows A and B evaluated as functions of l_{\max} in the range 1–50. It can be seen that to an excellent approximation,

$$\begin{aligned} A &= 1.401 + 0.626 \ln l_{\max}, \\ B &= 0.296 + 0.482 \ln l_{\max}. \end{aligned} \quad (73)$$

Clearly, both A and B diverge with increasing l_{\max} , implying a singularity in \tilde{T} at the X points. In fact, unphysical behavior is averted because Eq. (59) is *invalid* close to the X points. Note that the series (65) always converges for $y \neq 0$ because of the decaying exponential terms. Figure 5 shows contours of $\tilde{T} = -(y + |y| + \tilde{T})$ [see Eq. (61)] plotted in (y, μ) space, where \tilde{T} is evaluated from Eq. (65), with $l_{\max}=20$ (this is sufficient to ensure convergence everywhere except close to the X points). The flux surfaces lying inside the separatrix are at $y < 0$, the separatrix is at $y=0$, and the outer flux surfaces are at $y > 0$. The contours of \tilde{T} are consistent with heat flow from the X points to the outer region [assuming $T'_s < 0$; see Eq. (61)]. As expected, the temperature profile is flat in the region $y \ll -1$, and is a flux surface constant with nonzero cross surface gradient in the region $y \gg 1$.

C. The X-point region

Consider the region in the vicinity of the lower X point (i.e., $|\zeta| \ll W_c/W$). Let

$$\begin{aligned} y &= \frac{1}{2} \left(\frac{W_c}{W} \right)^2 z, \\ \zeta &= 2 \left(\frac{W_c}{W} \right)^2 \lambda, \end{aligned} \quad (74)$$

then Eq. (26) reduces to

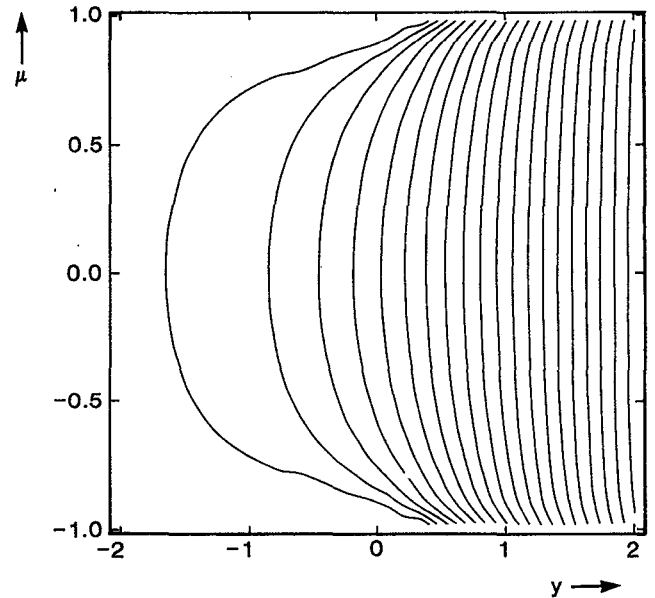


FIG. 5. Equally spaced contours of the temperature profile $\tilde{T}(y, \mu)$, which characterizes the temperature variation across the separatrix of a large magnetic island (see Sec. IV B). The profile increases monotonically with increasing y .

$$\frac{1}{4} \frac{\partial}{\partial \lambda} \sqrt{z + \lambda^2} \frac{\partial \tilde{T}}{\partial \lambda} + \frac{\partial}{\partial z} \sqrt{z + \lambda^2} \frac{\partial \tilde{T}}{\partial z} = 0. \quad (75)$$

Equation (75) can be transformed into the small $|\zeta|$ limit of Eq. (59), provided that $(W/W_c)^2 \gg |\lambda| \gg 1, \sqrt{|z|}$. It follows that (59) breaks down in the vicinity of the X points when

$$\sqrt{1 - \mu^2} \ll \left(\frac{W_c}{W} \right)^2 + \frac{W_c}{W} \sqrt{|y|}. \quad (76)$$

Note, in particular, that on the separatrix ($y=0$), Eq. (59) is invalid for $\sqrt{1 - \mu^2} \ll (W_c/W)^2$.

Suppose that²⁶

$$\begin{aligned} \xi &= |\lambda| + \sqrt{z + \lambda^2}, \\ \eta &= |\lambda| - \sqrt{z + \lambda^2}, \end{aligned} \quad (77)$$

then Eq. (75) transforms to

$$\mathcal{L}\tilde{T}(\xi, \eta) = 0, \quad (78)$$

where

$$\mathcal{L} \equiv \left(\xi \frac{\partial}{\partial \xi} - \eta \frac{\partial}{\partial \eta} \right)^2 + \left(\frac{\partial}{\partial \xi} - \frac{\partial}{\partial \eta} \right)^2. \quad (79)$$

The symmetry requirements (20) and (22) become

$$\tilde{T}(\xi, \eta) = -\tilde{T}(\eta, \xi) \quad (80)$$

for $\eta > 0$ (i.e., inside the separatrix), and

$$\tilde{T}(\xi, \eta) = \tilde{T}(-\eta, -\xi) \quad (81)$$

for $\eta < 0$ (i.e., outside the separatrix). The boundary conditions (60) and $\tilde{T} \rightarrow 0$ as $y \rightarrow -\infty$ transform to

$$\tilde{T}(\xi, \eta) \rightarrow -\frac{\pi}{8} W T'_s \left(\frac{W_c}{W} \right)^4 \xi \eta, \quad (82)$$

as $\xi\eta \rightarrow -\infty$, and $\tilde{T}/\xi\eta \rightarrow 0$ as $\xi\eta \rightarrow \infty$.

It is easily demonstrated that

$$\begin{aligned}\mathcal{L}(\xi\eta) &= -2, \\ \mathcal{L}[F(\xi)] &= \mathcal{L}[F(\eta)] = 0, \\ \mathcal{L}[F^2(\xi)] &= \mathcal{L}[F^2(\eta)] = 2,\end{aligned}\quad (83)$$

where

$$F(z) = \sinh^{-1} z \equiv \ln(z + \sqrt{1+z^2}). \quad (84)$$

It follows that

$$\tilde{T}(\xi, \eta) = T_1(\xi, \eta) + T_2(\xi, \eta) + C[F(\xi) - F(\eta)], \quad (85)$$

where C is an arbitrary constant. Here,

$$T_1(\xi, \eta) = -\frac{\pi}{16} WT'_s \left(\frac{W_c}{W}\right)^4 [2\xi\eta + F^2(\xi) + F^2(\eta)] \quad (86)$$

for $\eta < 0$, and

$$T_1(\xi, \eta) = -\frac{\pi}{16} WT'_s \left(\frac{W_c}{W}\right)^4 [F^2(\xi) - F^2(\eta)], \quad (87)$$

for $\eta > 0$, with $T_2(\xi, \eta)/\xi\eta \rightarrow 0$ as $|\xi\eta| \rightarrow \infty$, and

$$\begin{aligned}T_2(\xi, \eta = 0) &= 0, \\ \left(\frac{\partial T_2}{\partial \eta}\right)_{\eta=0+} &= -\frac{\pi}{8} WT'_s \left(\frac{W_c}{W}\right)^4 \xi.\end{aligned}\quad (88)$$

The function $T_2(\xi, \eta)$ must also satisfy the symmetry requirements (80) and (81).

D. Asymptotic matching

According to the previous section, the behavior of \tilde{T} on the separatrix ($\eta=0$) is given by

$$\begin{aligned}\tilde{T}(y=0, \xi) &= -\frac{\pi}{16} WT'_s \left(\frac{W_c}{W}\right)^4 \left\{ \sinh^{-1} \left[\left(\frac{W}{W_c}\right)^2 |\xi| \right] \right\}^2 \\ &+ C \sinh^{-1} \left[\left(\frac{W}{W_c}\right)^2 |\xi| \right],\end{aligned}\quad (89)$$

close to the lower X point. Thus, the asymptotic behavior of the X-point solution in the limit $\sqrt{1-\mu^2} \gg (W_c/W)^2$ becomes

$$\begin{aligned}\tilde{T}(y=0, \mu) &= -\frac{\pi}{16} WT'_s \left(\frac{W_c}{W}\right)^4 \left[\ln \sqrt{1-\mu^2} \right. \\ &+ 2 \ln \left(\frac{W}{W_c}\right) + 2 \ln 2 \left. \right]^2 \\ &+ C \left[\ln \sqrt{1-\mu^2} + 2 \ln \left(\frac{W}{W_c}\right) + 2 \ln 2 \right].\end{aligned}\quad (90)$$

The logarithmic singularities in Eq. (90) at $\mu = \pm 1$ are resolved for $\sqrt{1-\mu^2} \ll (W_c/W)^2$ in Eq. (89). The analysis of Sec. IV B can be corrected to take this into account by shifting the limits of integration in the variable μ from ± 1 to $\pm 1 \mp (W_c/W)^4$. It follows that each term on the left-hand side of Eq. (69) acquires a small correction of order

$(W_c/W)^4 \ln(W/W_c)$. These corrections are cumulative, and the net correction becomes of the order of the right-hand side when

$$l_{\max} \sim \left(\frac{W}{W_c}\right)^4 / \ln \left(\frac{W}{W_c}\right), \quad (91)$$

at which point the series is assumed to effectively truncate. It follows from Eqs. (71) and (73) that to lowest order the asymptotic behavior of the boundary layer solution in the limit $|\mu| \rightarrow 1$ is given by

$$\begin{aligned}\tilde{T}(y=0, \mu) &\rightarrow \frac{\pi}{8} WT'_s \left(\frac{W_c}{W}\right)^2 \times 2.5 \ln \left(\frac{W}{W_c}\right) \left[\ln \sqrt{1-\mu^2} \right. \\ &+ 1.93 \ln \left(\frac{W}{W_c}\right) \left. \right],\end{aligned}\quad (92)$$

where it is assumed that $\ln(W/W_c) \gg 1$.

In the limit $W/W_c \gg 1$, the asymptotic solutions (90) and (92) match up, provided

$$C = 0.98 WT'_s \left(\frac{W_c}{W}\right)^2 \ln \left(\frac{W}{W_c}\right). \quad (93)$$

The fact that there is only a small (3%) residual difference in the coefficient of $\ln(W/W_c)$ (inside the square bracket) between the two solutions, suggests that the truncation prescription (91) is essentially correct. Thus, to lowest order, the function \tilde{T} reduces to

$$\begin{aligned}\tilde{T}(\xi, \eta) &\approx 0.98 WT'_s \left(\frac{W_c}{W}\right)^2 \ln \left(\frac{W}{W_c}\right) \sinh^{-1}(\xi \sqrt{1+\eta^2}) \\ &- \eta \sqrt{1+\xi^2},\end{aligned}\quad (94)$$

in the X-point region (i.e., $|y| \ll 1$ and $\sqrt{1-\mu^2} \ll 1$).

E. Summary

The boundary layer region is sketched in Fig. 6. The layer is centered on the separatrix ($\Omega=1$), attaining a maximum width of order W_c in the vicinity of the X points, and a minimum width of order $(W_c)^2/W$ halfway between the X points. The layer expands in width as W_c approaches W , eventually allowing cross-flux surface temperature gradients to establish themselves inside the separatrix. The temperature gradients probably first appear in the X-point regions, and only reach the O points when $W_c \sim W$. Of course, for $W_c \gg W$ there is no flattening of the temperature profile (see Sec. III D).

The net heat flux flowing around the boundary layer is given by

$$Q_{\parallel}(\xi) = \int_{\Omega=1-}^{\Omega=1+} \frac{\mathbf{q} \cdot \hat{\mathbf{z}} \wedge \nabla \Omega}{|\nabla \Omega|} \frac{d\Omega}{|\nabla \Omega|}. \quad (95)$$

In the thin island limit ($W \ll r_s$), this expression reduces to

$$Q_{\parallel}(\xi) \approx \mp \frac{\pi}{2} \kappa_{\parallel} WT'_s \frac{(\mathbf{b} \cdot \nabla \xi)^2}{|\nabla \Omega| |\nabla \xi|} \left(\frac{W_c}{W}\right)^4 \frac{\partial}{\partial \xi} \int_{-\infty}^{\infty} \tilde{T}(y, \xi) dy, \quad (96)$$

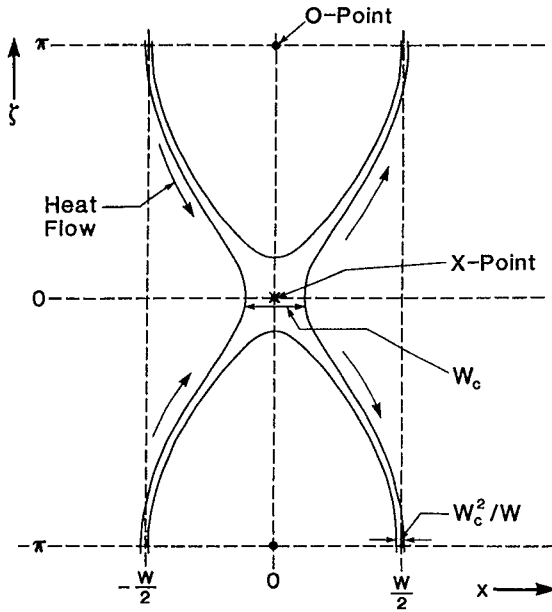


FIG. 6. Schematic diagram of the boundary region that transports heat across a large magnetic island. Here, x is the radial distance from the rational surface and ζ is the helical angle.

where use has been made of Eqs. (10), (58), and (61), and the upper/lower signs correspond to $x \gtrless 0$, respectively. Further analysis yields

$$Q_{\parallel}(\mu) \approx \pm \frac{\pi}{2} \frac{\kappa_{\perp}}{m} r_s T'_s (1 - \mu^2) \frac{\partial}{\partial \mu} \int_{-\infty}^{\infty} \tilde{T}(y, \mu) dy, \quad (97)$$

with the aid of Eqs. (8) and (27), where $\mu = \cos \zeta/2$. It follows from Eqs. (62), (65), (66), and the properties of Legendre functions, that

$$\int_{-\infty}^{\infty} \tilde{T}(y, \mu) dy = D + \ln(1 - \mu^2), \quad (98)$$

where D is an arbitrary constant. Thus,

$$Q_{\parallel}(\zeta) \approx \mp \frac{\pi}{m} \kappa_{\perp} r_s T'_s \cos \zeta/2. \quad (99)$$

Heat is channeled to each X-point region via two separatrix boundary layers, so the net heat flux flowing across a given X point ($\zeta=0$, say) in the $+r$ direction is

$$Q_{X \text{ point}} \approx - \frac{2\pi}{m} \kappa_{\perp} r_s T'_s. \quad (100)$$

The net heat flux flowing across magnetic flux surfaces outside the separatrix is given by

$$Q_{\perp} = \oint \frac{\mathbf{q} \cdot \nabla \Omega}{|\nabla \Omega|} \frac{d\zeta}{|\nabla \zeta|} \approx - \kappa_{\perp} \oint |\nabla \Omega| \frac{\partial \tilde{T}}{\partial \Omega} \frac{d\zeta}{|\nabla \zeta|}. \quad (101)$$

According to the analysis of Sec. III E, the cross-surface heat flux attains a constant steady-state value,

$$Q_{\perp} \approx - \frac{2\pi}{m} \kappa_{\perp} r_s T'_s. \quad (102)$$

A comparison of Eqs. (100) and (102) reveals that on the rational surface ($x=0$) the whole of the cross-surface heat flux flows through the X-point regions.

V. BOOTSTRAP-DRIVEN MAGNETIC ISLANDS

A. Introduction

One of the most important conclusions of neoclassical theory is that radial gradients in the plasma pressure can drive a noninductive "bootstrap" current parallel to the magnetic field when the plasma is sufficiently collisionless.²⁷ In fact, substantial bootstrap contributions to the equilibrium plasma current have been observed experimentally.^{28,29} The perturbed bootstrap current can, in principle, profoundly affect the stability of tearing modes.^{18,30} This effect is investigated in the following.

B. Analysis

In the vicinity of a constant- ψ magnetic island, the perturbed Ohm's law takes the form³¹

$$\frac{\partial \Psi}{\partial t} \cos \zeta + \mathbf{b} \cdot \nabla \phi = - \eta_z(r_s) (\delta j_z - \widetilde{\delta j_z}), \quad (103)$$

where ϕ is the perturbed electrostatic potential, $\eta_z(r)$ is the parallel resistivity, δj_z is the total perturbed parallel current, and $\widetilde{\delta j_z}$ is the noninductive part of the perturbed parallel current. The total current is related to the standard tearing stability index Δ' via

$$\begin{aligned} \Delta' &\equiv \left(\frac{d\psi}{dr} \right)_{r_{s-}}^{r_{s+}} / \Psi \\ &= - \frac{2}{\Psi} \oint \frac{d\zeta}{2\pi} \int_{r_{s-}}^{r_{s+}} \mu_0 \delta j_z \cos \zeta dr. \end{aligned} \quad (104)$$

It is helpful to define the flux surface average operator $\langle \cdots \rangle$, where

$$\langle f(\sigma, \Omega, \zeta) \rangle = \oint \frac{f(\sigma, \Omega, \zeta)}{\sqrt{\Omega - \cos \zeta}} \frac{d\zeta}{2\pi}, \quad (105)$$

for $\Omega > 1$, and

$$\langle f(\sigma, \Omega, \zeta) \rangle = \int_{\zeta_0}^{2\pi - \zeta_0} \frac{\frac{1}{2}[f(\sigma, \Omega, \zeta) + f(-\sigma, \Omega, \zeta)]}{\sqrt{\Omega - \cos \zeta}} \frac{d\zeta}{2\pi}, \quad (106)$$

for $\Omega \leq 1$. Here, $\sigma = \text{sgn}(x)$, $\zeta_0 = \cos^{-1} \Omega$, and f is a general function. It is easily demonstrated that

$$\langle \mathbf{b} \cdot \nabla f \rangle = 0 \quad (107)$$

[see Eqs. (8) and (15)]. Equations (104), (105), and (106) yield

$$\begin{aligned} \Delta' &= - \frac{\mu_0 W}{\sqrt{2} \Psi} \int_{-1}^{\infty} \left\langle \frac{1}{2} [\delta j_z(\sigma, \Omega, \zeta) \right. \\ &\quad \left. + \delta j_z(-\sigma, \Omega, \zeta)] \cos \zeta \right\rangle d\Omega. \end{aligned} \quad (108)$$

By definition, a “nonlinear” magnetic island has a much greater radial width than a linear layer. In conventional tokamaks the characteristic layer width is given by^{32,33}

$$\frac{\delta_{\text{layer}}}{r_s} \sim \left(\frac{\tau_H^2}{\tau_V \tau_R} \right)^{1/6}, \quad (109)$$

where $\tau_H = (R_0/B_z) \sqrt{\mu_0 \rho(r_s)/n s_s}$, $\tau_R = \mu_0 r_s^2 / \eta_z(r_s)$, and $\tau_V = r_s^2 \rho(r_s) / \mu_\perp(r_s)$ are the hydromagnetic, resistive, and viscous time scales at the rational surface, respectively. Here, $\rho(r)$ is the plasma mass density, and $\mu_\perp(r)$ is the (anomalous) perpendicular viscosity. It can be demonstrated that the perturbed current is a flux surface constant in the vicinity of a nonlinear island,¹⁶ so that

$$\delta j_z = \delta j_z(\Omega). \quad (110)$$

In fact, a viscous boundary layer of characteristic width $\sqrt{\delta_{\text{layer}}^3/W}$ develops on the separatrix in order to resolve the current and flow patterns for $\Omega \geq 1$ (cf. Sec. IV, where a similar boundary layer resolves the temperature profiles on either side of the separatrix).^{34,35} Note that the perturbed current is not necessarily a flux surface function for $W \lesssim \delta_{\text{layer}}$. It follows from Eqs. (9), (103), (107), (108), and (110) that the temporal evolution of a nonlinear island is governed by^{16,31}

$$I_1 \tau_R \frac{d}{dt} \left(\frac{W}{r_s} \right) = \Delta' r_s + \frac{16}{\sqrt{2}} \frac{r_s}{W} \frac{R_0 q_s}{B_z s_s} \times \int_{-1}^{\infty} \frac{\langle \mu_0 (\delta j_z)_+ \rangle \langle \cos \zeta \rangle}{\langle 1 \rangle} d\Omega, \quad (111)$$

where, $(\delta j_z)_+$ is that part of the perturbed noninductive current that is even across the rational surface, and³⁴

$$I_1 = \sqrt{2} \int_{-1}^{\infty} \frac{\langle \cos \zeta \rangle^2}{\langle 1 \rangle} d\Omega = 0.8227. \quad (112)$$

The perturbed bootstrap current satisfies³⁶

$$\widetilde{\delta j_z} \approx -1.46 \frac{q_s}{\sqrt{\epsilon_s} B_z} \frac{\partial \delta p_e}{\partial x}, \quad (113)$$

close to the rational surface, where $\delta p_e(x)$ is the perturbed electron pressure. Suppose, for the sake of simplicity, that the density and electron temperature profiles are similar in the island region (i.e., the ratios of the parallel to perpendicular transport coefficients are about the same for density and temperature—a more realistic model is discussed in Sec. VII). It follows that

$$\delta p_e(x) \approx \frac{p'_s}{T'_s} \delta T(x), \quad (114)$$

for the single fluid model adopted in this paper, where p'_s is the electron pressure gradient at the rational surface. In the small island limit ($W \ll W_c$), Eqs. (37), (113), and (114) imply that

$$\langle \widetilde{\delta j_z} \rangle \approx -0.438 \frac{q_s}{\sqrt{\epsilon_s} B_z} \left(\frac{W}{W_c} \right)^2 \langle \cos \zeta \rangle, \quad (115)$$

whereas in the large island limit ($W \gg W_c$) Eqs. (8), (41), (113), and (114) yield

$$\langle \widetilde{\delta j_z} \rangle \approx 1.46 \frac{q_s}{\sqrt{\epsilon_s} B_z} \frac{p'_s}{B_z} \langle 1 \rangle, \quad (116)$$

for $\Omega < 1$, and

$$\langle \widetilde{\delta j_z} \rangle \approx -1.62 \frac{q_s}{\sqrt{\epsilon_s} B_z} \frac{p'_s}{kE(1/k^2)} + 1.46 \frac{q_s}{\sqrt{\epsilon_s} B_z} \frac{p'_s}{B_z} \langle 1 \rangle, \quad (117)$$

for $\Omega \geq 1$, where $k = \sqrt{(1+\Omega)/2}$. Equations (111), (115), (116), and (117) give

$$I_1 \tau_R \frac{d}{dt} \left(\frac{W}{r_s} \right) \approx \Delta' r_s + 2.88 \sqrt{\epsilon_s} \frac{\beta'_s}{s_s} \frac{r_s W}{W_c^2} \quad (118)$$

in the small island limit, and

$$I_1 \tau_R \frac{d}{dt} \left(\frac{W}{r_s} \right) \approx \Delta' r_s + 9.25 \sqrt{\epsilon_s} \frac{\beta'_s}{s_s} \frac{r_s}{W} \quad (119)$$

in the large island limit, where

$$\beta'_s = - \left(\frac{q_s}{\epsilon_s} \right)^2 \frac{\mu_0 r_s p'_s}{B_c^2} \quad (120)$$

is a measure of the equilibrium pressure gradient. Note that β'_s is typically of the order of the poloidal beta. In the above, use has been made of the results,

$$\int_{-1}^{\infty} \langle \cos \zeta \rangle d\Omega = 0 \quad (121)$$

and

$$\int_1^{\infty} \frac{\langle \cos \zeta \rangle}{\langle 1 \rangle} \frac{d\Omega}{kE(1/k^2)} = 0.5054. \quad (122)$$

C. Discussion

According to Eqs. (118) and (119), the nonlinear island width evolution equation can be written as

$$I_1 \tau_R \frac{d}{dt} \left(\frac{W}{r_s} \right) \approx \Delta' r_s + \Delta_{\text{boot}}(W), \quad (123)$$

where

$$\Delta_{\text{boot}}(W) \approx 4.63 \sqrt{\epsilon_s} \frac{\beta'_s}{s_s} \frac{r_s W}{W_d^2} \frac{2}{1 + (W/W_d)^2}, \quad (124)$$

with $W_d \approx 1.8 W_c$ [see Eq. (27)]. Clearly, for conventional tokamak plasma profiles (i.e., $p'_s < 0$ and $s_s > 0$), the perturbed bootstrap current has a *destabilizing* effect on magnetic islands. The destabilizing term $\Delta_{\text{boot}}(W)$ initially increases with island width, reaching a maximum value,

$$\Delta_{\text{max}} \approx 4.63 \sqrt{\epsilon_s} \frac{\beta'_s}{s_s} \frac{r_s}{W_d} \quad (125)$$

at $W = W_d$, and then starts to decrease. The nonmonotonic behavior of the destabilizing term comes about because the

finite parallel thermal conductivity of the plasma effectively sets an upper limit on the perturbed pressure gradient in the island region.

Suppose, for the sake of simplicity, that the variations of Δ' with island width are relatively unimportant. It is easily demonstrated that magnetic islands decay away to zero width when $\Delta' r_s < -\Delta_{\max}$. For $-\Delta_{\max} \leq \Delta' r_s < 0$, there is a critical island width,

$$W_- = W_d(\lambda - \sqrt{\lambda^2 - 1}) \leq W_d, \quad (126)$$

where $\lambda = \Delta_{\max}/(-\Delta' r_s)$. Islands whose widths are less than the critical value decay away, whereas islands whose widths exceed the critical value are maintained in the plasma by the perturbed bootstrap current and eventually attain the steady-state width,

$$W_+ = W_d(\lambda + \sqrt{\lambda^2 - 1}) \geq W_d. \quad (127)$$

The scale length W_d is the minimum steady-state island width, which can be maintained in the plasma by the perturbed bootstrap current. It is concluded that *an intrinsically stable magnetic island* (i.e., $\Delta' < 0$) *cannot be destabilized by the perturbed bootstrap current alone* (assuming, of course, that the calculated value of W_d is significantly greater than the linear layer width): some other effect is required to force the island width above the critical value.

In the presence of an m/n field error, the evolution equation for a *locked* island is written³⁵ as

$$I_1 \tau_R \frac{d}{dt} \left(\frac{W}{r_s} \right) \approx \Delta' r_s + \Delta_{\text{boot}}(W) + 2m \left(\frac{W_v}{W} \right)^2, \quad (128)$$

where W_v is the vacuum island width associated with the external perturbation. Here, it is assumed that there is relatively little plasma current outside the rational surface. In the absence of bootstrap effects, the steady-state width of the error field-driven island is given by

$$W_c = \sqrt{\frac{2m}{-\Delta' r_s}} W_v. \quad (129)$$

Suppose $\lambda \gg 1$, so that $W_- \approx W_d/2\lambda$ and $W_+ \approx 2\lambda W_d$. It is easily demonstrated from Eq. (128) that as W_c is gradually increased from a small value, there is a *bifurcation* of the steady-state island width, from $(\frac{2}{3})W_-$ to W_+ , when

$$W_c \geq (W_c)_{\text{crit}} \approx \frac{2}{3\sqrt{3}} W_-. \quad (130)$$

Clearly, in this situation a *small* error field can trigger the growth of a *large* magnetic island. The final island is much larger than the purely error field-driven island, and is maintained in the plasma principally by the perturbed bootstrap current. This effect may offer an explanation for some puzzling experimental results recently obtained on (the Joint European Torus) JET.³⁷ It is found that the critical threshold amplitude for the phase locking of a driven island by an error field (and, hence, for substantial driven magnetic reconnection in the plasma) is consistent with established theory,³⁸ but that after locking the final island width is much larger (by up to an order of magnitude) than expected. This effect is not observed in low β_p plasmas.³⁹ It is speculated that the rela-

tively low locking threshold expected for (the International Tokamak Experimental Reactor) ITER,³⁵ coupled with the relatively high expected β_p (and, hence, strong bootstrap effects), will lead to a stringent upper limit on the tolerable level of error fields (typically, $b_{\text{error}}/B_z \sim 2 \times 10^{-5}$). If this limit is exceeded, the error fields will *lock* the plasma and induce small error field-driven islands, which will then *trigger* substantial bootstrap-driven magnetic islands. This process is likely to severely degrade the plasma performance, and may even lead to a major disruption.^{37,39,40}

VI. IMPLICATIONS FOR OHMICALLY HEATED TOKAMAKS

The parallel thermal conductivity takes the form¹⁷

$$\kappa_{\parallel} \sim n_e v_e \lambda_e, \quad (131)$$

in a short mean-free path plasma, where n_e is the electron number density, v_e is the electron thermal velocity, and λ_e is the electron mean-free path. However, in a conventional tokamak plasma, the mean-free path λ_e typically *exceeds* the parallel wavelength $\lambda_{\parallel} = 1/|k_{\parallel}|$ of helical perturbations. The simple-minded application of Eq. (131) yields unphysically large parallel heat fluxes. The parallel conductivity in the physically relevant long mean-free path limit ($\lambda_e \gg \lambda_{\parallel}$) is crudely estimated as

$$\kappa_{\parallel} \sim n_e v_e \lambda_{\parallel}, \quad (132)$$

which is equivalent to replacing conduction by convection (i.e., $n_e v_{\parallel} \nabla_{\parallel} T$) in the heat flow equation (13). For a magnetic island of width W , the typical value of λ_{\parallel} is $n_s W/R_0$.

Perpendicular energy transport in tokamaks is highly anomalous, probably due to the action of *short-wavelength* electrostatic drift waves.⁴¹ It is, therefore, appropriate to use the *anomalous* perpendicular transport coefficient to study the physics of long-wavelength (low mode number) magnetic islands. Assuming, for the sake of simplicity, that κ_{\perp} is approximately constant across the plasma, it is easily demonstrated that³⁵

$$\kappa_{\perp} \sim \frac{n_e a^2}{6 \tau_E}, \quad (133)$$

where τ_E is the global (anomalous) energy confinement time scale.

Consider the simple scaling model for Ohmically heated tokamak plasmas outlined in Ref. 33. The aspect ratio is $a = 0.35 R_0$, the toroidal magnetic field strength scales like $B_z(T) = 1.38 R_0^{0.7}$ (m), the pressure profile is parabolic, the central temperature is estimated by balancing the Ohmic heating power against anomalous losses calculated using the neo-Alcator energy confinement time scale,⁴² and deuterium is the fueling ion species. The central q is 0.7, the edge q is 4.5, and the line-averaged electron number density is $2 \times 10^{19} \text{ m}^{-3}$. For the 2/1 mode, $r_s = 0.66a$ and $s_s = 1.74$. Table I shows the ratio of parallel to perpendicular thermal conductivities at the $q=2$ surface, the critical island width W_d (for the 2/1 mode), and the parameter Δ_{\max} (for the 2/1 mode), estimated as functions of the major radius using this scaling model.

TABLE I. The ratio of parallel to perpendicular thermal conductivities, the scale island width W_d , and the parameter Δ_{\max} , estimated as functions of the major radius (for the 2/1 mode) using a simple scaling model for Ohmically heated plasmas.

R_0 (m)	$\kappa_{\parallel}/\kappa_{\perp}$	W_d/a	Δ_{\max}
0.50	6.4×10^6	0.105	3.8
0.75	2.4×10^7	0.076	4.8
1.00	6.2×10^7	0.060	5.6
1.50	2.3×10^8	0.043	6.9
2.00	6.6×10^8	0.033	8.1
3.00	2.4×10^9	0.024	9.5
4.00	6.2×10^9	0.019	10.7
6.00	2.5×10^{10}	0.013	13.3
8.00	6.0×10^{10}	0.011	13.8

It can be seen from Table I that the ratio of parallel to perpendicular conductivities increases rapidly with increasing machine size, giving rise to a corresponding reduction in the scale island width W_d . Recall [from Eq. (27) and Sec. V C] that W_d is the minimum steady-state island width that can be maintained in the plasma by the perturbed bootstrap current. For island widths less than W_d , bootstrap effects attenuate rapidly because the *finite* parallel thermal conductivity of the plasma limits the perturbed pressure gradient that can develop in the vicinity of the island. In particular, there is no flattening of the plasma pressure inside the separatrix for $W \ll W_d$. In small tokamaks W_d is typically about 10% of the minor radius, suggesting that only large magnetic islands are capable of flattening the temperature profile. Conversely, in large tokamaks W_d falls to a few percent of the minor radius, suggesting that small to medium islands can modify the temperature profile. The quantity Δ_{\max} , which is the peak destabilizing bootstrap contribution to the Rutherford island equation [see Eq. (125)], increases slowly with an increasing major radius, but is significant for both large and small devices.

VII. CONCLUSIONS

The electron temperature perturbations associated with tearing modes are investigated for typical tokamak plasma parameters. It is found that there is a critical island width W_d below which the conventional scenario where the temperature is flattened inside the island separatrix breaks down due to the stagnation of magnetic field lines (i.e., $\mathbf{b} \cdot \nabla \sim 0$) in the vicinity of the rational surface and the finiteness of the plasma parallel thermal conductivity. The critical width is easily estimated as the distance from the rational surface at which the two terms in the heat diffusion equation (13) balance. Thus,

$$\kappa_{\parallel}(\mathbf{b} \cdot \nabla)^2 \sim \kappa_{\perp}(\nabla_{\perp})^2,$$

giving [see Eqs. (15)]

$$\kappa_{\parallel}(ns_s/R_0r_s)^2(W_d)^2 \sim \kappa_{\perp}/(W_d)^2,$$

and so

$$\frac{W_d}{r_s} \sim \left(\frac{\kappa_{\perp}}{\kappa_{\parallel}} \right)^{1/4} \left(\frac{1}{\epsilon_s s_s n} \right)^{1/2},$$

where R_0 is the plasma major radius, r_s is the minor radius of the rational surface, $\epsilon_s = r_s/R_0$ is the local inverse aspect ratio, s_s is the local magnetic shear, and n is the toroidal mode number. The critical width is non-negligible in conventional tokamak plasmas (see Table I). Islands whose widths are much less than W_d give rise to no local flattening of the electron temperature profile. Such islands have very different ECE signatures to conventional magnetic islands. In principle, it should be possible to differentiate the two types of magnetic island using ECE data and, thereby, determine W_d experimentally. It should also be possible to map out the outer ideal MHD eigenfunctions using ECE temperature measurements.

Nonzero temperature gradients inside large magnetic islands have recently been observed on the Rijnhuizen tokamak RTP.⁴³ Furthermore, a mismatch between the island width deduced from magnetic data and that obtained from electron temperature measurements has been seen on the Wendelstein VII-A stellarator.⁴⁴ In both cases, these effects are plausibly explained in terms of field line stagnation and a large, but finite, ratio of parallel and perpendicular thermal conductivities in the plasma.

Islands whose widths are much less than W_d are not significantly destabilized by the perturbed bootstrap current, unlike conventional magnetic islands. It seems, therefore, unlikely that bootstrap effects alone could destabilize an intrinsically stable ($\Delta' < 0$) magnetic island. Some other effect is required to force the island width above W_d . In principle, the growth of bootstrap-driven islands could be triggered by coupling to other modes (via toroidicity and flux surface shaping) or interaction with external perturbations. Such coupling or interaction is known to destabilize tearing modes, but becomes ineffective below a certain threshold mode amplitude due to the naturally occurring differential rotation present in tokamak plasmas.^{35,45} It is concluded that under normal circumstances (i.e., in the absence of mode locking) intrinsically stable tearing modes (i.e., virtually all tearing modes) are not unduly affected by the perturbed bootstrap current. However, once mode locking has occurred (triggered, for instance, by the growth of an intrinsically unstable mode, an increased error field amplitude, or a reduction in the plasma viscosity due to a fall in plasma density) the growth of bootstrap-driven islands could be enabled (see Sec. V C). This mechanism offers a plausible explanation for some recent JET results, in which mode locking induced by a static error field (triggered by a drop in the plasma density) give rise to the formation of unexpectedly large static magnetic islands.³⁷ There are no islands present in the plasma prior to mode locking, and, in most cases, island formation eventually leads to a major disruption. Similar undesirable behavior can probably only be avoided in the proposed ITER device if the level of field errors is kept well below the critical value required to induce mode locking (i.e., $b_{\text{error}}/B_z \lesssim 2 \times 10^{-5}$).³⁵

In this paper it is assumed that the island lies in a region where there are no significant sources (or sinks) of heat, so that $\nabla \cdot \mathbf{q} = 0$. This is a reasonable assumption, but there are, nevertheless, situations in which it is not appropriate. For instance, when electron cyclotron radio frequency heating

(ECRH) is tuned so that the resonance lies close to the rational surface. Localized heating of the island region gives rise to two quite separate effects. The first effect is due to local modification of the *equilibrium* current profile, and can be either stabilizing or destabilizing.⁴⁶ The second, and far stronger, effect is due to the interaction of the localized power input with the *helical* structure of the island, and depends crucially on the temperature being a flux surface function in the vicinity of the island.³¹ For islands whose width is much less than the critical width W_d , the second effect disappears, whereas the first effect persists.

Finally, it should be noted that the arguments used in this paper to investigate *energy* transport could just as well be applied to *particle* transport. For example, by analogy with Eq. (13), a particle diffusion equation can be written as

$$D_{\parallel} \nabla_{\parallel}^2 n_e + D_{\perp} \nabla_{\perp}^2 n_e = 0.$$

Thus, all of the results of Sec. II onward also apply to the *density* perturbations associated with tearing modes, provided that $\kappa_{\parallel}/\kappa_{\perp}$ is replaced by D_{\parallel}/D_{\perp} in the analysis. In particular, there is a critical island width,

$$\frac{W_{d'}}{r_s} \sim \left(\frac{D_{\perp}}{D_{\parallel}} \right)^{1/4} \left(\frac{1}{\epsilon_s s n} \right)^{1/2},$$

below which the density profile is not flattened inside the separatrix. In conventional tokamak plasmas, $n_e D_{\perp} \sim \kappa_{\perp}$ and $n_e D_{\parallel} \sim \sqrt{m_e/m_i} \kappa_{\parallel}$, where m_e is the electron mass and m_i the fueling ion mass.^{8,17} In fact, in the long mean-free path regime $n_e D_{\parallel} \sim (m_e/m_i)^{3/2} \kappa_{\parallel}$ because of the dependence of D_{\parallel} and κ_{\parallel} on island width—see Eq. (132). For the Ohmically heated tokamak plasmas investigated in Table I (with deuterium as the fueling ion species) $D_{\parallel}/D_{\perp} \sim 4.2 \times 10^{-3} \kappa_{\parallel}/\kappa_{\perp}$, which implies that $W_{d'} \sim 3.9 W_d$. It follows from Table I that flattening of the density profile by magnetic islands is only likely to occur for relatively large islands in big tokamaks, and is unlikely to occur at all in small tokamaks. Note that only the largest magnetic islands, with $W \gg W_{d'}$ or W_d , experience the full destabilizing influence of the perturbed bootstrap current. Medium-sized islands, $W_{d'} \gg W \gg W_d$, only experience that part of the bootstrap effect that is due to perturbed temperature gradients, and small islands, $W \ll W_d$ experience no effect whatsoever.

ACKNOWLEDGMENTS

The author would like to thank A. J. Wootton, G. Cima, and H. Gasquet (Fusion Research Center, The University of Texas, Austin), R. D. Hazeltine (Institute for Fusion Studies, The University of Texas, Austin), J. D. Hanson (Auburn University), C. C. Hegna (University of Wisconsin), R. J. Hastie (Culham Laboratory), and A. Reiman (Princeton Plasma Physics Laboratory), for helpful discussions during the preparation of this paper.

¹J. A. Wesson, *Tokamaks*, edited by J. A. Wesson (Clarendon, Oxford, 1987), Chap. 7.

²S. V. Mironov and I. B. Semenov, *At. Energ.* **30**, 20 (1971) [*Sov. J. At. Energy* **30**, 22 (1971)].

³J. A. Wesson, R. D. Gill, M. Hugon, F. C. Schüller, J. A. Snipes, D. J. Ward, D. V. Bartlett, D. J. Campbell, P. A. Duperrex, A. W. Edwards, R. S. Granetz, N. A. O. Gottardi, T. C. Hender, E. Lazzaro, P. J. Lomas, N.

Lopes Cardozo, K. F. Mast, M. F. F. Nave, N. A. Salmon, P. Smeulders, P. R. Thomas, B. J. D. Tubbing, M. F. Turner, and A. Weller, *Nucl. Fusion* **29**, 641 (1989).

⁴H. P. Furth, J. Killeen, and M. N. Rosenbluth, *Phys. Fluids* **6**, 459 (1963).

⁵R. R. Dominguez and R. E. Waltz, *Nucl. Fusion* **27**, 65 (1987); Z. Chang and J. D. Callen, *ibid.* **30**, 219 (1990).

⁶J. A. Snipes, D. J. Campbell, T. C. Hender, M. von Hellermann, and H. Weisen, *Nucl. Fusion* **30**, 205 (1990).

⁷R. B. White, in *Handbook of Plasma Physics* (North-Holland, Amsterdam, 1983), Vol. 1, Sec. 3.5.

⁸J. W. Connor, in Ref. 1, Chap. 4.

⁹J. Y. Chen, S. C. McCool, A. J. Wootton, A. Y. Aydemir, M. E. Austin, R. D. Bengtson, R. V. Bravenec, D. L. Brower, R. M. Denton, M. S. Foster, H. Lin, N. C. Luhmann, Jr., S. M. Mahajan, A. Ouroua, W. A. Peebles, P. E. Phillips, B. Richards, C. P. Ritz, P. M. Schoch, W. L. Rowan, B. A. Smith, X. Z. Yang, C. X. Xu, Y. Z. Zhang, and Z. M. Zhang, in *Research Using Small Tokamaks*, Proceedings of the Technical Committee Meeting, Arlington, 1990 (International Atomic Energy Agency, Vienna, 1990), p. 41.

¹⁰O. Klüber, H. Zohm, H. Bruhns, J. Gernhardt, A. Kallenbach, and H. P. Zehrfeld, *Nucl. Fusion* **31**, 907 (1991).

¹¹A. E. Costley, in Ref. 1, Chap. 10.

¹²A. W. Edwards, D. J. Campbell, W. W. Engelhardt, H. U. Fahrback, R. D. Gill, R. S. Granetz, S. Tsuji, B. J. D. Tubbing, A. Weller, J. A. Wesson, and D. Zasche, *Phys. Rev. Lett.* **57**, 211 (1986).

¹³Y. Nagayama, K. M. McGuire, M. Bitter, A. Cavallo, E. D. Fredrickson, K. W. Hill, H. Hsuan, A. Janos, W. Park, G. Taylor, and M. Yamada, *Phys. Rev. Lett.* **67**, 3527 (1991).

¹⁴J. A. Wesson, in Ref. 1, Chap. 3.

¹⁵J. A. Wesson, in Ref. 1, Chap. 6.

¹⁶P. H. Rutherford, *Phys. Fluids* **16**, 1903 (1973).

¹⁷S. I. Braginskii, in *Reviews of Plasma Physics* (Consultants Bureau, New York, 1965), Vol. 1, p. 205.

¹⁸C. C. Hegna and J. D. Callen, *Phys. Fluids B* **4**, 1855 (1992).

¹⁹M. Kotschenreuther, R. D. Hazeltine, and P. J. Morrison, *Phys. Fluids* **28**, 294 (1985).

²⁰L. M. Milne-Thomson, *Handbook of Mathematical Functions*, edited by M. Abramowitz and I. A. Stegun (Dover, New York, 1965), Chap. 17.

²¹M. C. Zarnstorff, S. Batha, A. Janos, F. L. Levinton, and the TFTR Group, in *Local Transport Studies in Fusion Plasmas*, Proceedings of Workshop, Varenna 1993 (Società Italiana di Fisica, Bologna, 1993), p. 257.

²²J. D. Callen, Z. Cheng, R. L. Coffey, T. A. Gianakon, C. C. Hegna, A. J. Smolyakov, W. X. Qu, and J. P. Wong, in Ref. 21, p. 243.

²³I. A. Stegun, in Ref. 20, Chap. 8.

²⁴A. Erdélyi, *Higher Transcendental Functions* (McGraw-Hill, New York, 1953), Chap. III.

²⁵P. J. Davis, in Ref. 20, Chap. 6.

²⁶D. Edery, M. Frey, J. P. Somon, M. Tagger, J. L. Soule, R. Pellat, and M. N. Bussac, *Phys. Fluids* **26**, 1165 (1983).

²⁷R. J. Bickerton, J. W. Connor, and J. B. Taylor, *Nature* **229**, 110 (1971).

²⁸R. J. Hawryluk, V. Arunasalam, M. G. Bell, M. Bitter, W. R. Blanchard, N. L. Bretz, R. Bundy, C. E. Bush, J. D. Callen, S. A. Cohen, S. K. Combs, S. L. Davis, D. L. Dimock, H. F. Dylla, P. C. Efthimion, L. C. Emerson, A. C. England, H. P. Eubank, R. J. Fonck, E. Fredrickson, H. P. Furth, G. Gammel, R. J. Goldston, B. Grek, L. R. Grisham, G. Hammett, H. Hsuan, R. A. Hulse, K. P. Jaehnig, D. Jassby, F. C. Jobes, D. W. Johnson, L. C. Johnson, R. Kaita, R. Kamperschroder, S. M. Kaye, S. J. Kilpatrick, R. J. Knize, H. Kugel, P. H. LaMarche, B. LeBlanc, R. Little, C. H. Ma, D. M. Manos, D. K. Mansfield, R. T. McCann, M. P. McCarthy, D. C. McCune, K. McGuire, D. H. McNeill, D. M. Meade, S. S. Medley, D. R. Mikkelsen, S. L. Milora, W. Morris, D. Mueller, V. Mukhovatov, E. B. Nieschmidt, J. O'Rourke, D. K. Owens, H. Park, N. Pomphrey, B. Prichard, A. T. Ramsey, M. H. Redi, A. L. Roquemore, P. H. Rutherford, N. R. Sauthoff, G. Schilling, J. Schivell, G. L. Schmidt, S. D. Scott, S. Sesnic, J. C. Sinnis, F. J. Stauffer, B. C. Stratton, G. D. Tait, G. Taylor, J. R. Timberlake, H. H. Townner, M. Ulrickson, V. Vershkov, S. von Goeler, F. Wagner, R. Wieland, J. B. Wilgen, M. Williams, K. L. Wong, S. Yoshikawa, R. Yoshino, K. M. Young, M. C. Zarnstorff, V. S. Zaveriaev, and S. J. Zweben, in *Plasma Physics and Controlled Nuclear Fusion Research 1986*, Proceedings of the 11th International Conference, Kyoto 1986 (International Atomic Energy Agency, Vienna, 1987), Vol. 1, p. 51.

²⁹C. D. Challis, J. G. Cordey, H. Hammen, P. M. Stubberfield, J. P. Christiansen, E. Lazzaro, D. G. Muir, D. Stork, and E. Thompson, *Nucl. Fusion* **29**, 563 (1989).

- ³⁰R. Carrera, R. D. Hazeltine, and M. Kotschenreuther, *Phys. Fluids* **29**, 899 (1986).
- ³¹P. H. Rutherford, in *Basic Physical Processes of Toroidal Fusion Plasmas*, Proceedings of Course and Workshop, Varenna 1985 (Commission of the European Communities, Brussels, 1986), Vol. 2, p. 531.
- ³²A. Bondeson and J. R. Sorbel, *Phys. Fluids* **27**, 2028 (1984).
- ³³R. Fitzpatrick, *Phys. Plasmas* **1**, 3308 (1994).
- ³⁴R. Fitzpatrick and T. C. Hender, *Phys. Fluids B* **3**, 644 (1991).
- ³⁵R. Fitzpatrick, *Nucl. Fusion* **33**, 1049 (1993).
- ³⁶M. N. Rosenbluth, R. D. Hazeltine, and F. L. Hinton, *Phys. Fluids* **15**, 116 (1972).
- ³⁷G. M. Fishpool and P. S. Haynes, *Nucl. Fusion* **34**, 109 (1994).
- ³⁸R. Fitzpatrick, in *Theory of Fusion Plasmas*, Proceedings of the Joint Varenna–Lausanne International Workshop, Varenna 1992 (Società Italiana di Fisica, Bologna, 1992), p. 147.
- ³⁹T. C. Hender, R. Fitzpatrick, A. W. Morris, P. G. Carolan, R. D. Durst, T. Edlington, J. Ferreira, S. J. Fielding, P. S. Haynes, J. Hugill, I. J. Jenkins, R. J. La Haye, B. J. Parham, D. C. Robinson, T. N. Todd, M. Valović, and G. Vayakis, *Nucl. Fusion* **32**, 2091 (1992).
- ⁴⁰J. T. Scoville, R. J. La Haye, A. G. Kellman, T. H. Osborne, R. D. Stambaugh, E. J. Strait, and T. S. Taylor, *Nucl. Fusion* **31**, 875 (1991).
- ⁴¹A. J. Wootton, W. Dorland, and M. Kotschenreuther (private communication, 1994).
- ⁴²W. W. Pfeiffer and R. E. Waltz, *Nucl. Fusion* **19**, 51 (1979).
- ⁴³B. P. van Milligen, A. C. A. P. van Lammerden, N. J. Lopes Cardozo, F. C. Schüler, and M. Verreck, *Nucl. Fusion* **33**, 1121 (1993).
- ⁴⁴R. Jaenicke and the Wendelstein VII-A Team, *Nucl. Fusion* **28**, 1737 (1988).
- ⁴⁵R. Fitzpatrick, R. J. Hastie, T. J. Martin, and C. M. Roach, *Nucl. Fusion* **33**, 1533 (1993).
- ⁴⁶E. Westerhof, *Nucl. Fusion* **27**, 1929 (1987).